NIH Public Access
Author Manuscript
Invest Ophthalmol Vis Sci. Author manuscript; available in PMC 2010 May 17.

Published in final edited form as:
Invest Ophthalmol Vis Sci. 2009 July ; 50(7): 3283–3290. doi:10.1167/iovs.08-3052.

αB-crystallin: A Golgi-Associated Membrane Protein in the Developing Ocular Lens

Rajendra K. Gangalum[1] and **Suraj P. Bhat**[1,2,3]

[1]Jules Stein Eye Institute, Geffen School of Medicine, University of California School of Medicine, Los Angeles, California.

[2]Brain Research Institute, University of California School of Medicine, Los Angeles, California.

[3]Molecular Biology Institute, University of California School of Medicine, Los Angeles, California.

Abstract

Purpose—All crystallins have non-crystallin catalytic functions. Because catalytic functions do not require large concentrations of protein, as are seen in the lens, there is a perception of dichotomy in the catalytic/physiological function of crystallins within and outside the lens. The status of αB-crystallin, a ubiquitously expressed small heat shock protein (and a crystallin) in the ocular lens, was investigated.

Methods—Discontinuous sucrose density gradients were used for fractionation of Golgi membranes and vesicles. Light microscopy and confocal microscopy were used for immunolocalization in cultured cells and the native lens.

Results—αB-crystallin is highly organized, as indicated by its polar presence in the apical Golgi in lens epithelium and in the perinuclear Golgi streaks in differentiating lens fiber cells. Assessment of the distribution of αB-crystallin in Golgi-enriched and vesicular fractions (characterized by the presence of Golgi membrane protein GM130 and vesicle coat protein γCOP) in the developing lens reveal a gradual transition from Golgi to vesicular fraction, concomitant with the appearance of αB-crystallin as a "soluble" protein.

Conclusions—These data demonstrate that αB-crystallin, known to be a soluble protein, starts life as a Golgi-associated membrane protein in the fetal and early postnatal lens and that the developmentally controlled physical state of the Golgi determines the status of this protein in the lens. These findings also show the similarity in the localization/ physiological function of αB-crystallin within and outside the ocular lens and suggest that non-crystallin/catalytic function is an innate component of the expression of a crystallin in the lens.

The small heat shock protein αB-crystallin is ubiquitous in the eukaryotic ocular lens. In addition to its expression in the lens, where it is known to be a subunit of the lens protein α-crystallin, this protein is part of the normal biologic and pathologic compositions of a number of nontransparent tissues.[1–3] Its expression has been shown to be associated with various non-crystallin (nonrefractive) phenotypes, ranging from cancer and cardiomyopathy to neurodegenerative disorders such as Alzheimer's disease, Parkinson's disease, and multiple sclerosis.[1] At the molecular level, αB-crystallin has anti-aggregation properties, binding to

© Association for Research in Vision and Ophthalmology

Corresponding author: Suraj P. Bhat, 100 Stein Plaza, BH623, Jules Stein Eye Institute, UCLA School of Medicine, Los Angeles, CA 90095; bhat@jsei.ucla.edu..

Disclosure: **R.K. Gangalum**, None; **S.P. Bhat**, None

Supported by the National Institutes of Health (SPB). SPB is a Wasserman Merit Scholar (Research to Prevent Blindness Inc.).

NIH-PA Author Manuscript
NIH-PA Author Manuscript
NIH-PA Author Manuscript

NIH-PA Author Manuscript

NIH-PA Author Manuscript

NIH-PA Author Manuscript

partially denatured polypeptides in vitro.[3] At the cellular level, it is present in the cell nucleus,[4,5] it has anti-apoptotic properties, and it is reported to associate with cytoskeletal elements.[1,6–9] It interacts with caspase 3[10] and with proteosomal subunit C8/α7,[11] and it is reported to be part of the SCF (Skp1/Cul1/F-box) ligase complex that degrades cyclin D.[12,13] Whether any of these associations or functions are relevant to lens physiology remain to be elucidated.

The development of the ocular lens and the emergence of the phenotype of transparency are associated with high concentrations of proteins (crystallins); all crystallins in the ocular lens, including αB-crystallin, are considered soluble structural proteins. Crystallins are also expressed in non-transparent tissues, albeit at comparatively low levels, where they perform catalytic, nonrefractive, non-crystallin functions considered irrelevant to their function in the lens. The perception thus prevails that catalytic, non-crystallin functions of crystallins are extraneous to the lens,[14,15] and whether crystallins have relevant non-crystallin functions within the lens is a question that has remained unanswered. One of the primary reasons this question has not been addressed is that the non-crystallin/catalytic functions of these proteins are unknown. Among major crystallins, more is known about the non-crystallin functions and associations of αB-crystallin.[6] We have recently discovered that in the human glioblastoma cell line U373, αB-crystallin localizes to Golgi in a cell cycle–dependent fashion,[16] suggesting a Golgi-related function for this protein. We have exploited this Golgi association of αB-crystallin in U373 cells as a conceptual and experimental rationale to address this question by examining the status of this protein in the developing rat ocular lens. The findings presented here provide insight into the distribution of a crystallin within a specific cellular compartment of the differentiating fiber cell and suggest developmental control of protein distribution through its non-crystallin function.

Materials and Methods

Animals and Antibodies

Sprague-Dawley rats (Charles River Laboratories, Wilmington, MA) were used in accordance with the guidelines of the ARVO Statement for the Use of Animals in Ophthalmic and Vision Research and the Animal Research Committee of the University of California at Los Angeles. Antibodies used for immunoblotting included rabbit polyclonal antibody 16 to αB-crystallin (dilution 1:5000; Sigma-Genosys, St. Louis, MO), mouse monoclonal antibody to GM130 (1:1000; BD Bio-sciences, Lexington, KY) and rabbit polyclonal antibodies to γCOP (1:500), cytochrome *c* (1:2000), and Calnexin (1:2000; Santa Cruz Biotechnology Inc., Santa Cruz, CA). For αB and GM130 detection, goat anti–rabbit antibody (1:250,000) and goat anti–mouse secondary antibodies (1:5000; Pierce, Rockford, IL), respectively, were used. For all primary antibodies obtained from Santa Cruz Biotechnology, peroxide-coupled goat anti–rabbit horseradish peroxidase secondary anti-body was used (1:20,000). For immunofluorescence studies with lens epithelial cell primary cultures, rabbit polyclonal anti–αB-crystallin (1:100 dilution) and goat anti–rabbit secondary antibody coupled to TRITC (tetramethylrhodamine isothiocyanate red; 1:200) and mouse monoclonal primary antibody GM130/FITC (fluorescein isothiocyanate; 1:100) were used.

Discontinuous Sucrose Density-Gradient Fractionation and Immunoblotting

Postnuclear homogenates were prepared from whole lenses or various dissected lens regions (see Figs. 1, 3, and 5). Discontinuous sucrose density gradients were run as reported previously.[16] This gradient generates a Golgi-enriched membrane fraction (S2) and a heavier vesicular fraction (S3; Fig. 3, insets). The gradient was collected dropwise (approximately 100 μL per fraction) from the bottom, and aliquots were analyzed by immunoblotting. For comparison of the Golgi membrane fraction and the vesicular fraction at different developmental ages (see

NIH-PA Author Manuscript

NIH-PA Author Manuscript

NIH-PA Author Manuscript

Fig. 8), the two fractions—Golgi (S2) and vesicular (S3)—were collected directly by piercing through the wall of the tube with a syringe.

Brefeldin-A Treatment

Fresh postnatal day (P)10 rat eyes were washed with phosphate-buffered saline (PBS) and were incubated in a CO_2 incubator at 37°C in 200 μL of Eagle minimum essential medium with Earle salts containing 10% fetal bovine serum, 1% L-glutamine, and 1% penicillin and streptomycin (MEM NEAA complete; Irvine Scientific, Santa Ana, CA) in the presence or absence of Brefeldin A (BFA; 1 μg/mL; Fluka, Switzerland) for 90 minutes. The lenses were rinsed with PBS before further pro-cessing.

Immunofluorescence with Cell Cultures

P10 rat lens epithelial explants were cultured in six-well plates (in MEM NEAA complete) for 6 to 8 days, and medium was replaced every 48 hours. Cells obtained from these cultures were seeded on poly-L-lysine (Sigma-Aldrich, St. Louis, MO)–coated microscope coverslips (Fisher Scientific, CA), allowed to grow for 24 hours, fixed, and processed for immunofluorescence.[16] Images were acquired as *z*-stacks (0.5-μm thick) with a confocal microscope (100× objective; TCS-SP Multiphoton; Leica, Wetzlar, Germany) and were processed with image processing software (Photoshop 6.0; Adobe, San Jose, CA).

*α*B-crystallin Immunolocalization in the Ocular Lens

Freshly dissected P10 rat eyes were briefly immersed in PBS (1×) and were fixed in 4% paraformaldehyde overnight at 4°C. For immunolocalization, 5-μm–thick paraffin sections were deparaffinized, rehydrated, and washed with PBS. Nonspecific sites were blocked with PBS containing 1% BSA, 5% goat serum, and 0.2% Triton X-100, processed for immunofluorescence with the use of anti–αB-crystallin and goat anti–rabbit secondary antibody-FITC (green),[16] and were incubated with *N*-((4-(4,4-difluoro-5-(2-thienyl)-4-bora-3a,4a-diaza-*s*-indacene-3-yl)-phenoxy)acetyl)sphingosine (BODIPY TR ceramide; Invitrogen, Carlsbad, CA) for 45 minutes.[17] DAPI (4′,6-diamidino-2-phenylindole) was used to stain the nuclei. Sections were imaged with a confocal microscope (10× objective; TCS SP; Leica; see Fig. 6) or a diagnostics camera (40× objective; Eclipse E800 with Spot Diagnostics; Nikon, Tokyo, Japan; see Fig. 7).

Results

*α*B-crystallin in Perinuclear Golgi

The ocular lens of the vertebrate eye is a cellular structure.[18] It consists of two well-defined morphologic and physiological compartments, the epithelium and the fiber cells (Fig. 1). Primary rat lens epithelial cell cultures were established and analyzed for immunolocalization with anti–αB-crystallin and an antibody against GM130, a Golgi matrix protein.[19] αB-crystallin colocalizes with GM130 within the perinuclear Golgi in the resting and recently divided cells (Fig. 2A). Similar results were obtained with cell cultures derived from bovine lens epithelium (Gangalum RK, Bhat SP, unpublished observations, 2007). These data establish that αB-crystallin localizes to the perinuclear Golgi, both in human glioblastoma cell line U373, as previously reported,[16] and in primary cultures of lens epithelial cells. Interestingly, these cell cultures contain elongated fiber-like cells. Based on our previous experience,[20] we presumed these to be fiber cells. One of these cells is shown in Figure 2B. Fiber cells are produced by the differentiation of lens epithelial cells; thus, the origin of these cells could be epithelial cells on their way to differentiation or fiber cells contaminating these cultures. Notwithstanding the origin of this fiberlike cell, the physiognomy of the Golgi, as revealed by the colocalization of αB-crystallin and GM130, is remarkable (Fig. 2B). The

NIH-PA Author Manuscript

NIH-PA Author Manuscript

NIH-PA Author Manuscript

location of the Golgi, in close juxtaposition to the nucleus, very much like a perinuclear envelope, is significant. In comparison, the Golgi in the circular, undifferentiated epithelial cells is confined to a perinuclear spot (Fig. 2B, round epithelial cell). In light of these findings it was important to examine the native lens.

αB-crystallin Fractionates with the Golgi Membranes

Figure 3A shows the distribution of αB-crystallin in a discontinuous sucrose density gradient[21] that was used to fractionate a postnuclear extract made from fetal day (FD) 18 whole lenses. The presence of GM130 in fractions 9 to 12 establishes the position of Golgi membranes (fraction S2) and a vesicular fraction (fractions 3–5, S3; Fig. 3, inset). Almost all αB-crystallin is associated with the S2 fraction. Considering that αB-crystallin is known to be a soluble crystallin, this is a highly significant observation. There is an insignificant contribution to this pattern by mitochondrial (cytochrome *c*)[22] and endoplasmic reticulum (ER; Calnexin [Santa Cruz Biotechnology]) markers.[23] We further ascertained the identity of these two fractions (S2 and S3) by electron microscopy (Gangalum RK, Bhat SP, unpublished observations, 2008). The S2 fraction is composed of tubular membranous structures, whereas the S3 fraction is composed of smaller vesicles, conforming to the previously established content of these fractions.[24,25]

The experiment described was repeated with P10 and P20 lenses. Figure 3B shows data obtained with P20 lens dissected into two anatomic regions, the E+SC and the FM. In E+SC, αB-crystallin is seen predominantly in Golgi membrane fractions (Fig. 3B). However, the distribution of αB-crystallin in the P20 FM (Fig. 3B) is more diffuse, similar to that obtained with P10 whole lens (Gangalum RK, Bhat SP, unpublished observations, 2007) showing more αB-crystallin in the top of the gradient. The pattern obtained with P20 FM also shows αB-crystallin further down in the gradient, nearer vesicular fractions (fractions 3–5), in stark contrast to that in the fetal (Fig. 3A, FD18) and E+SC gradients (Fig. 3B), suggesting that lens αB-crystallin is associated with protein-rich membranous structures derived from the Golgi. This is supported by the suscep-tibility of the sucrose density-gradient patterns to BFA, a fungal antibiotic that disrupts the Golgi organization.[16,26] Pretreatment of the lenses with BFA, before fractionation, shifts the pattern of αB-crystallin distribution to the top of the gradient, suggesting release of this protein from the Golgi membranes (Fig. 4; compare +BFA and –BFA). In comparison, BFA treatment does not show any significant impact on the distribution of the mitochondrial marker cytochrome *c*.

To further investigate the regional status of the distribution of αB-crystallin and its association with Golgi, we dissected the P20 lens into three anatomic compartments: the epithelium and the adhered superficial cortex (E+SC) as described (Fig. 3B), the differentiating region or BR, and the remaining FM (Fig. 5; inset). The postnuclear supernatant from each of these anatomic regions was examined on independent gradients (Fig. 5). Similar amounts of protein from each gradient were used for immunoblotting to allow meaningful comparison. Notably, the distribution of αB-crystallin was more discrete, and there was similarity in the patterns obtained. Based on quantitative immunoblotting (Gangalum RK, Bhat SP, unpublished observations, 2008), we calculated that in BR, approximately 70% of αB-crystallin in the postnuclear homogenate was associated with the Golgi-enriched (S2) fraction.

αB-crystallin in the Native Lens

Unlike cultured cells, ocular lens cells do not stain with many available Golgi protein markers because the processing regimen for microscopy invariably impacts the Golgi membrane integrity, making it difficult to pick up low-concentration Golgi proteins. Figures 6A and 6B show confocal images of immunolocalized αB-crystallin in the lens epithelium and differentiating BR, respectively, of a P10 rat lens. αB-Crystallin shows remarkable polarity

NIH-PA Author Manuscript

NIH-PA Author Manuscript

NIH-PA Author Manuscript

and is seen localized in apical, perinuclear Golgi in the epithelial layer (Fig. 6A). These data confirm the polar localization of αB-crystallin in Golgi seen in cultured lens epithelial cells (Fig. 2A). A similar pattern was observed with peroxidase and diaminobenzidine staining (Gangalum RK, Bhat SP, unpublished observations, 2007). Figure 6A also shows thin anteroposterior streaks of αB-crystallin staining in the FM of the lens. This becomes clearer in Figure 6B, which shows the equatorial region of the lens.

Examination of the equatorial/bow region of the P10 lens shows αB-crystallin–stained long perinuclear streaks of Golgi (green) running alongside the elongated nuclei (blue; Fig. 7). These data establish that the polarity of the perinuclear presence of the Golgi and, therefore, αB-crystallin is also maintained in differentiating fiber cells. That the green streaks, seen in Figure 7, represent Golgi is based on the specificity of staining of Golgi by anti–αB-crystallin (Figs. 2, 6, 7) and previous work,[16] on their perinuclear location, and on staining by silver nitrate impregnation, a method used previously by others[28] to stain Golgi in ocular tissues (Gangalum RK, Bhat SP, unpublished observations, 2007).

αB-crystallin as a Probe of Golgi Status during Lens Growth and Maturation

We believe that the diffuse pattern of αB-crystallin distribution seen in Figure 3B (P20, FM), compared with that seen in the fetal lens (Fig. 3A, FD18) and younger fiber cells in the P20 lens (Fig. 3B, E+SC), is related to increased degradation (including the generation of vesicles) of the Golgi in terminally differentiating fiber cells in older lenses. Based on this thesis, therefore, when studied temporally, we must see a transition of the distribution of αB-crystallin from the Golgi to vesicles derived from it. This is exactly what we see in Figure 8. Postnuclear extracts made from lenses of different ages were fractionated with the same gradients used for analyses in Figures 3 to 5.

From FD18 to P5, little of the three proteins (GM130, γCOP,[26] αB-crystallin) is found in the S3 fraction, suggesting that scant Golgi is represented in the vesicular population. All three proteins are seen in the S2 (Golgi) fraction. In these early stages, a robust S2 fraction (Golgi) is present. The absence of these proteins in the S3 fraction indicates that our experimental manipulations do not generate detectable S3 components in the presence of robust Golgi (S2 fraction; Fig. 8B). As the lens gets older, the amount of S3 fraction seems to increase (P10 – adult). By P20, the proportion of vesicles increases, as indicated by increased amounts of GM130, γCOP, and αB-crystallin in the S3 fraction, pointing to the breakdown of Golgi as the lens grows. In the adult lens only αB-crystallin is clearly detectable; GM130 and γCOP amounts are drastically decreased.

Discussion

This investigation makes three important observations. One is that the location of the Golgi determines the location of αB-crystallin in the developing lens. Another is that the physical state of Golgi in the ocular lens determines the status of the protein αB-crystallin (membrane bound or soluble). Yet another is that αB-crystallin associates with the Golgi in transparent and in nontransparent cells/tissues.

Our understanding of how ocular lens transparency comes about is based on extrapolations made from physical properties of highly concentrated protein (crystallin) solutions without the biological constraint that attends their biogenesis. It is significant that αB-crystallin, known to be a soluble protein, is a Golgi membrane-associated protein, indicating a commonality in the catalytic, non-crystallin function of this protein, outside and inside the ocular lens. These data provide a biological basis for the observations, made initially more than a quarter century ago, [29–31] about the association of α-crystallin polypeptides (αA and αB) with lens membranes. In light of our data, the reported association of αB-crystallin with the lens plasma membrane[32],

NIH-PA Author Manuscript

NIH-PA Author Manuscript

NIH-PA Author Manuscript

[33] suggests that Golgi is involved in the distribution of this protein in a developmentally dictated fashion.

The data presented in Figures 3, 4, and 8 provide important insight into the developmental history of the status of Golgi in the lens, as viewed through the patterns of αB-crystallin distribution. During fetal development (FD18), the lens is largely composed of the epithelium and early differentiating fiber cells, the stage at which Golgi is intact; therefore, most αB-crystallin fractionates with the Golgi membranes (Fig. 3A, top panel). This is similar to patterns obtained with the E+SC, the younger differentiating areas of the postnatal P20 lens (Fig. 3B). On the other hand, the FM in P20 (Fig. 3B) is composed of terminally differentiating fiber cells, which contain degenerating Golgi, in different states of disassembly, resulting in increased vesicular fraction (fractions 3–5) at the bottom of the gradient and soluble αB-crystallin at the top of the gradient. Most of the early studies involving lens α-crystallins were conducted with mature lenses, which would explain why only a fraction of αB-crystallin was associated with the membrane.[9,29,32] It is clear that the membrane presence of αB-crystallin stems from its developmental association with the Golgi complex. This may be so for other heat shock proteins, including Hsp27.[34] Preliminary data suggest that the other α-crystallin, αA-crystallin, shows differential association with the Golgi and lens membranes (Gangalum RK, Bhat SP, unpublished observations, 2008); this finding requires an independent investigation.

Although Golgi and vesicular structures in the ocular lens have been reported as early as 1958[35–38] and more recently by other investigators,[39–41] their relationship to crystallin distribution in the context of fiber cell differentiation has not been explored. The polarity of Golgi and, therefore, αB-crystallin in the lens epithelium (Figs. 2, 6A) suggests a specific physiological function for this protein. This polarity must also be considered in the context of epithelial fiber cell interface and reported molecular communication between the two cell types.[42] Interestingly, this polarity is also maintained in the fiber cells, where the protein is concentrated in the perinuclear streaks of Golgi, indicating that αB-crystallin is not simply accumulated as a soluble protein in the presumed cytoplasmic pool of crystallins, negating the common belief that lens cells are crystallin-crammed bags.

The morphologic transformation of the epithelial cell into differentiating fibers and the consequent terminal differentiation entails significant rearrangement of the membrane and protein components.[2,33,40,41,43,44] These molecular rearrangements must be consistent with the realization of the phenotype of transparency; any malfunction in this process could have pathologic consequences for transparency.[45,46] It is possible that Golgi is involved in these processes because the extensive presence of Golgi is seen along the anterior-posterior axes of differentiating fiber cells (Figs. 6B, 7).

An examination of the equatorial region shows a lack of staining in the bow area, where lens epithelial cells enter the differentiating zone (Fig. 6B, asterisk). This lack of staining may be related to fragmentation and reorganization of the Golgi that may attend the transition from the undifferentiated epithelium to differentiating fiber cells. Interestingly, however, immediately following the nonstained area is an area of intense staining of Golgi streaks (by anti–αB-crystallin) parallel to the long axis of the lens (Figs. 6B, 7), suggesting reconstitution/reorganization of the Golgi. In synchronized cultures of U373 human glioblastoma cells, Golgi association of αB-crystallin follows the cell cycle, and its reappearance in the daughter cell Golgi is coincident with the beginning of cytokinesis.[16] Thus, the bow region and the differentiating fiber cells may present an attractive paradigm for investigating the molecular progression that accompanies Golgi assembly and reorganization.[47–51]

NIH-PA Author Manuscript

NIH-PA Author Manuscript

NIH-PA Author Manuscript

In the ocular lens, degeneration of cellular organelles, including the Golgi and the nuclei, attends terminal differentiation of fiber cells.[38,40] The close association of Golgi and the differentiating fiber cell nuclei (Figs. 2B, 7) compels speculation of a causal link between the status of the Golgi and nuclear apoptosis.[50,52] Molecular cues that drive these processes and the function of αB-crystallin in the Golgi remain to be understood. It is, however, clear that non-crystallin properties of αB-crystallin, as inferred here from its location in a specific cellular compartment, are an important component of the biological progression that culminates in the emergence of the phenotype of transparency.[53]

Acknowledgments

The authors thank Mathew Schibler for his guidance and help with confocal microscopy and Joseph Horwitz and Michael Hall for reading the manuscript and making suggestions.

References

1. Bhat SP. Crystallins, genes and cataract. Prog Drug Res 2003;60:205–262. [PubMed: 12790344]
2. Bloemendal H, de Jong W, Jaenicke R, Lubsen NH, Slingsby C, Tardieu A. Ageing and vision: structure, stability and function of lens crystallins. Prog Biophys Mol Biol 2004;86:407–485. [PubMed: 15302206]
3. Horwitz J. Alpha-crystallin. Exp Eye Res 2003;76:145–153. [PubMed: 12565801]
4. Bhat SP, Hale IL, Matsumoto B, Elghanayan D. Ectopic expression of alpha B-crystallin in Chinese hamster ovary cells suggests a nuclear role for this protein. Eur J Cell Biol 1999;78:143–150. [PubMed: 10099937]
5. van Rijk AE, Stege GJ, Bennink EJ, May A, Bloemendal H. Nuclear staining for the small heat shock protein αB-crystallin colocalizes with splicing factor SC35. Eur J Cell Biol 2003;82:361–368. [PubMed: 12924631]
6. Andley UP. Crystallins in the eye: function and pathology. Prog Retin Eye Res 2007;26:78–98. [PubMed: 17166758]
7. Ghosh JG, Houck SA, Clark JI. Interactive sequences in the stress protein and molecular chaperone human αB crystallin recognize and modulate the assembly of filaments. Int J Biochem Cell Biol 2007;39:1804–1815. [PubMed: 17590381]
8. Kato K, Ito H, Inaguma Y, Okamoto K, Saga S. Synthesis and accumulation of αB crystallin in C6 glioma cells is induced by agents that promote the disassembly of microtubules. J Biol Chem 1996;271:26989–26994. [PubMed: 8900185]
9. Bloemendal H, Berbers GA, de Jong WW, et al. Interaction of crystallins with the cytoskeletal-plasma membrane complex of the bovine lens. CIBA Found Symp 1984;106:177–190. [PubMed: 6568972]
10. Kamradt MC, Chen F, Cryns VL. The small heat shock protein alpha B-crystallin negatively regulates cytochrome c- and caspase-8-dependent activation of caspase-3 by inhibiting its autoproteolytic maturation. J Biol Chem 2001;276:16059–16063. [PubMed: 11274139]
11. Boelens WC, Croes Y, de Jong WW. Interaction between alphaB-crystallin and the human 20S proteasomal subunit C8/alpha7. Biochim Biophys Acta 2001;1544:311–319. [PubMed: 11341940]
12. den Engelsman J, Keijsers V, de Jong WW, Boelens WC. The small heat-shock protein alpha B-crystallin promotes FBX4-dependent ubiquitination. J Biol Chem 2003;278:4699–4704. [PubMed: 12468532]
13. Barbash O, Lin DI, Diehl JA. SCF Fbx4/alphaB-crystallin cyclin D1 ubiquitin ligase: a license to destroy. Cell Div 2007;2:2. [PubMed: 17224055]
14. Wistow G, Piatigorsky J. Recruitment of enzymes as lens structural proteins. Science 1987;236:1554–1556. [PubMed: 3589669]
15. Wistow GJ, Piatigorsky J. Lens crystallins: the evolution and expression of proteins for a highly specialized tissue. Annu Rev Biochem 1988;57:479–504. [PubMed: 3052280]
16. Gangalum RK, Schibler MJ, Bhat SP. Small heat shock protein alphaB-crystallin is part of cell cycle-dependent Golgi reorganization. J Biol Chem 2004;279:43374–43377. [PubMed: 15339919]

NIH-PA Author Manuscript

NIH-PA Author Manuscript

NIH-PA Author Manuscript

17. Zhang Y, Lemasters J, Herman B. Secretory group IIA phospholipase A(2) generates anti-apoptotic survival signals in kidney fibroblasts. J Biol Chem 1999;274:27726–27733. [PubMed: 10488115]
18. Piatigorsky J. Lens differentiation in vertebrates: a review of cellular and molecular features. Differentiation 1981;19:134–153. [PubMed: 7030840]
19. Nakamura N, Rabouille C, Watson R, et al. Characterization of a cis-Golgi matrix protein, GM130. J Cell Biol 1995;131:1715–1726. [PubMed: 8557739]
20. Nagineni CN, Bhat SP. Human fetal lens epithelial cells in culture: an in vitro model for the study of crystallin expression and lens differentiation. Curr Eye Res 1989;8:285–291. [PubMed: 2707044]
21. Slusarewicz P, Nilsson T, Hui N, Watson R, Warren G. Isolation of a matrix that binds medial Golgi enzymes. J Cell Biol 1994;124:405–413. [PubMed: 8106542]
22. Wibo M, Thinès-Sempoux D, Amar-Costesec A, Beaufay H, Godelaine D. Analytical study of microsomes and isolated subcellular membranes from rat liver, VIII: subfractionation of preparations enriched with plasma membranes, outer mitochondrial membranes, or Golgi complex membranes. J Cell Biol 1981;89:456–474. [PubMed: 7251662]
23. Stankewich MC, Tse WT, Peters LL, et al. A widely expressed *β*III spectrin associated with Golgi and cytoplasmic vesicles. Proc Natl Acad SciUSA 1998;95:14158–14163.
24. Taylor RS, Jones SM, Dahl RH, Nordeen MH, Howell KE. Characterization of the Golgi complex cleared of proteins in transit and examination of calcium uptake activities. Mol Biol Cell 1997;8:1911–1931. [PubMed: 9348533]
25. Morgado-Díaz JA, Nakamura CV, Agrellos OA, et al. Isolation and characterization of the Golgi complex of the protozoan *Trypanosoma cruzi*. Parasitology 2001;123:33–43. [PubMed: 11467781]
26. McMahon HT, Mills IG. COP and clathrin-coated vesicle budding: different pathways, common approaches. Curr Opin Cell Biol 2004;16:379–391. [PubMed: 15261670]
27. Zhang Y, Lemasters J, Herman B. Localization of rat liver group IIA phospholipase A(2) in secretory pathways: green fluorescent protein approach. Microsc Microanal 2000;6:150–155. [PubMed: 10742402]
28. Garcia-Porrero JA, Icardo JM, Ojeda JL. A quantitative study of the position of the Golgi apparatus in the early developing chick eye. Anat Embryol (Berl) 1981;163:77–85. [PubMed: 7316225]
29. Kibbelaar MA, Bloemendal H. Fractionation of the water-soluble proteins from calf lens. Exp Eye Res 1979;29:679–688. [PubMed: 544284]
30. Deretic D, Abersold RH, Morrison HD, Papermaster DS. Alpha A- and alpha B-crystallin in the retina: association with the post-Golgi compartment of frog retinal photoreceptors. J Biol Chem 1994;269:16853–16861. [PubMed: 8207008]
31. Cobb BA, Petrash JM. Characterization of alpha-crystallin-plasma membrane binding. J Biol Chem 2000;275:6664–6672. [PubMed: 10692476]
32. Bagchi M, Gordon PA, Alcalá JR, Maisel H. The plasma membrane of the rabbit lens cortical fiber, I: isolation, characterization, and biosynthesis of two membrane intrinsic polypeptides. Invest Ophthalmol Vis Sci 1979;18:562–569. [PubMed: 447458]
33. Wang X, Garcia CM, Shui YB, Beebe DC. Expression and regulation of alpha-, beta-, and gamma-crystallins in mammalian lens epithelial cells. Invest Ophthalmol Vis Sci 2004;45:3608–3619. [PubMed: 15452068]
34. Preville X, Mehlen P, Fabre-Jonca N, et al. Biochemical and immunofluorescence analysis of the constitutively expressed HSP27 stress protein in monkey CV-1 cells. J Biosci 1996;21:221–234.
35. Wanko T, Gavin MA. The fine structure of the lens epithelium: an electron microscopic study. AMA Arch Ophthalmol 1958;60:868–879. [PubMed: 13582331]
36. Omulecka D. The Golgi apparatus in the eye tissues. Rocz Akad Med Im Juliana Marchlewskiego Bialymst Suppl 1965;12:5–76. [PubMed: 5216773]
37. Gorthy WC, Snavely MR, Berrong ND. Some aspects of transport and digestion in the lens of the normal young adult rat. Exp Eye Res 1971;12:112–119. [PubMed: 5120340]
38. Kuwabara T, Imaizumi M. Denucleation process of the lens. Invest Ophthalmol 1974;13:973–981. [PubMed: 4430579]
39. Yao R, Crossland W, Maisel H. Electron microscopic detection of glycoconjugates in the chicken lens. Exp Eye Res 1996;63:705–711. [PubMed: 9068377]

NIH-PA Author Manuscript

NIH-PA Author Manuscript

NIH-PA Author Manuscript

40. Bassnett S. Lens organelle degradation. Exp Eye Res 2002;74:1–6. [PubMed: 11878813]
41. Lo WK, Wen XJ, Zhou CJ. Microtubule configuration and membranous vesicle transport in elongating fiber cells of the rat lens. Exp Eye Res 2003;77:615–626. [PubMed: 14550404]
42. Rae JL, Bartling C, Rae J, Mathias RT. Dye transfer between cells of the lens. J Membr Biol 1996;150:89–103. [PubMed: 8699483]
43. Zigman S, Paxhia T, Marinetti G, Girsch S. Lipids of human lens fiber cell membranes. Curr Eye Res 1984;3:887–896. [PubMed: 6467965]
44. Zelenka PS. Lens lipids. Curr Eye Res 1984;3:1337–1359. [PubMed: 6391828]
45. Spector A, Garner MH, Garner WH, Roy D, Farnsworth P, Shyne S. An extrinsic membrane polypeptide associated with high-molecular-weight protein aggregates in human cataract. Science 1979;204:1323–1326. [PubMed: 377484]
46. Bloemendal H. Proctor lecture: disorganization of membranes and abnormal intermediate filament assembly lead to cataract. Invest Ophthalmol Vis Sci 1991;32:445–455. [PubMed: 2001920]
47. Seemann J, Pypaert M, Taguchi T, Malsam J, Warren G. Partitioning of the matrix fraction of the Golgi apparatus during mitosis in animal cells. Science 2002;295:848–851. [PubMed: 11823640]
48. Altan-Bonnet N, Sougrat R, Liu W, Snapp EL, Ward T, Lippincott-Schwartz J. Golgi inheritance in mammalian cells is mediated through endoplasmic reticulum export activities. Mol Biol Cell 2006;17:990–1005. [PubMed: 16314396]
49. Barr FA. Golgi inheritance: shaken but not stirred. J Cell Biol 2004;164:955–958. [PubMed: 15051731]
50. Machamer CE. Golgi disassembly in apoptosis: cause or effect? Trends Cell Biol 2003;13:279–281. [PubMed: 12791290]
51. Rossanese OW, Glick BS. Deconstructing Golgi inheritance. Traffic 2001;2:589–596. [PubMed: 11555412]
52. Nakagomi S, Barsoum MJ, Bossy-Wetzel E, Sütterlin C, Malhotra V, Lipton SA. A Golgi fragmentation pathway in neurodegeneration. Neurobiol Dis 2008;29:221–231. [PubMed: 17964175]
53. Bhat SP. Transparency and non-refractive functions of crystallins—a proposal. Exp Eye Res 2004;79:809–816. [PubMed: 15642317]

NIH-PA Author Manuscript
NIH-PA Author Manuscript
NIH-PA Author Manuscript

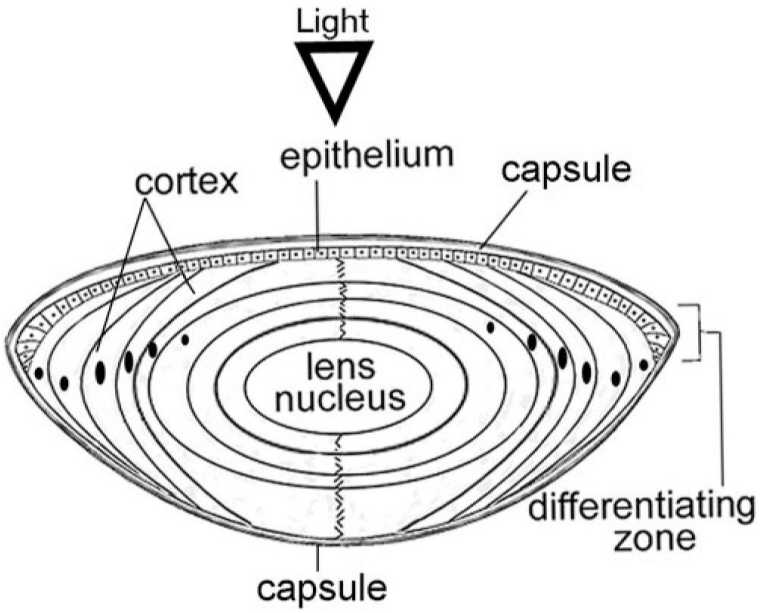

Figure 1.

Schematic of a cross-section of the ocular lens. The lens is surrounded by a basement membrane (capsule). A single layer of epithelial cells overlays the anterior surface of the lens. The bulk of the lens is made of concentric layers of highly elongated fiber cells that contain high concentrations of crystallins. Fiber cells are derived from the edges of the epithelial layer through a process of differentiation that takes place in the lens equator, also known as the bow region (BR) because of the characteristic pattern of the anteriorly displaced nuclei in the differentiating zone. The lens grows throughout life; thus, cells in the center (lens nucleus) are the oldest whereas cells nearer the surface are the youngest.[18] Terminal differentiation of fiber cells in the center (nucleus) is attended by loss of cellular organelles, including mitochondria, Golgi, and nuclei. In all experiments except in Figure 5, the lens epithelium and the superficial cortex (E+SC) were combined and analyzed separately from the rest of the lens fiber mass (FM).

NIH-PA Author Manuscript
NIH-PA Author Manuscript
NIH-PA Author Manuscript

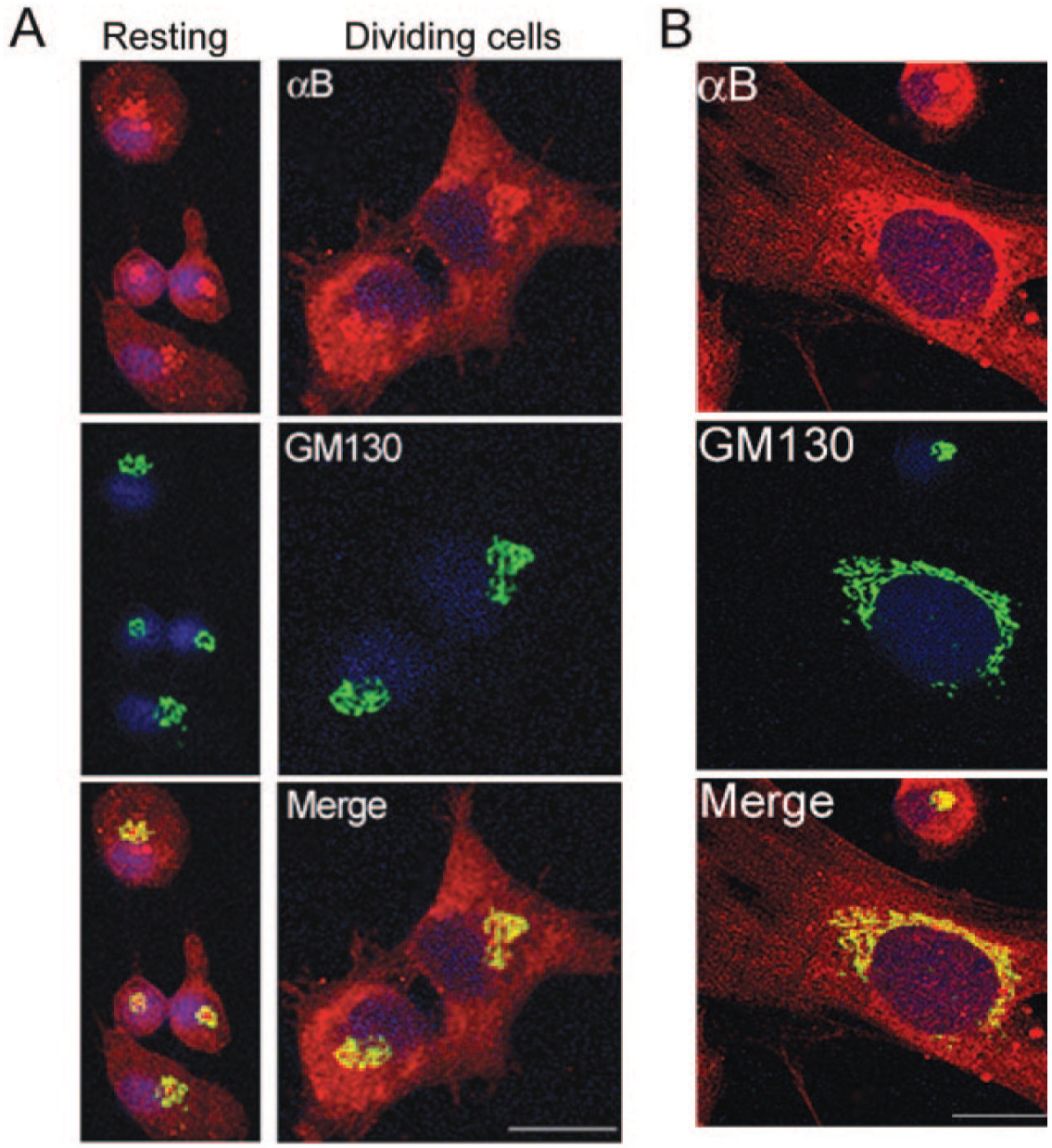

Figure 2.
*α*B-crystallin and GM130 colocalize in the perinuclear Golgi in primary cultures of rat lens epithelial cells. Confocal images of the primary cultures of P10 rat lens epithelial cells processed for immunolocalization with anti–*α*B-crystallin (*red*) and anti–GM130-FITC (*green*) are shown. Nuclei are labeled with DAPI (*blue*). (**A**, *left*) Resting cells. *Right*: dividing cells. (**B**) Crescent-shaped perinuclear Golgi in an elongated fiberlike cell in primary cultures of lens epithelial cells. Note the undifferentiated round cell on the top. Scale bar, 20 *μ*m.

NIH-PA Author Manuscript
NIH-PA Author Manuscript
NIH-PA Author Manuscript

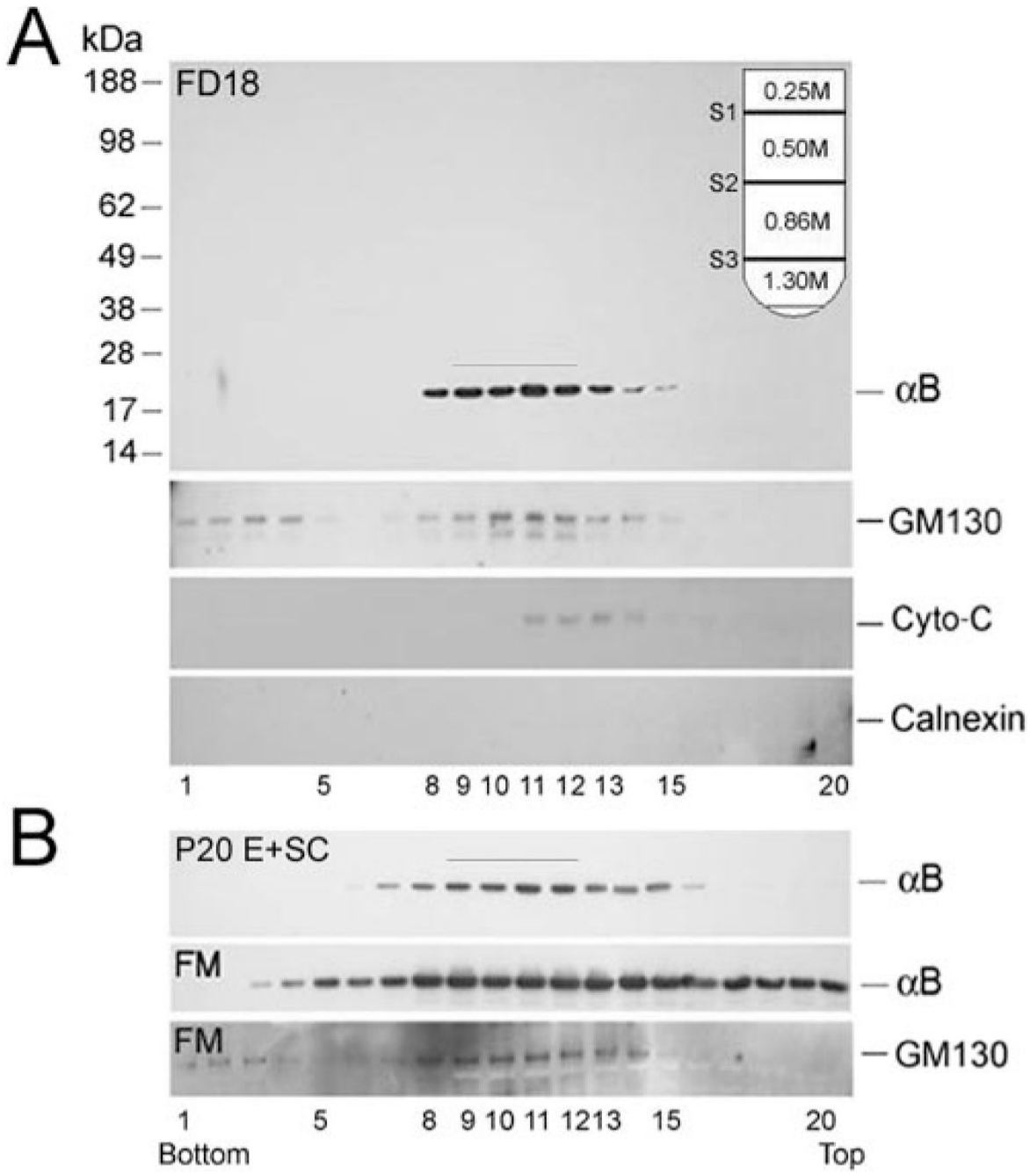

Figure 3.

*α*B-crystallin fractionates as a Golgi membrane- associated protein. (**A**) Distribution of *α*B-crystallin in FD18 whole lens postnuclear extracts (5.3 mg protein; *top*), fractionated on discontinuous density sucrose gradient (*inset*). (**B**) Distribution of *α*B-crystallin in postnuclear homogenates of E+SC (5.29 mg protein) and FM (6.53 mg protein) of P20 lens. For anti–*α*B-crystallin immunoblots, 1 *μ*L was used from each fraction; for the rest, 10 *μ*L were used. In the FD18 lens and the E+SC of the P20 lens, *α*B-crystallin predominantly fractionates with the Golgi membranes (fractions 9–12, bar). A whole immunoblot with molecular mass standards (kDa) is shown in FD18 panel; only relevant areas are shown in other panels.

NIH-PA Author Manuscript
NIH-PA Author Manuscript
NIH-PA Author Manuscript

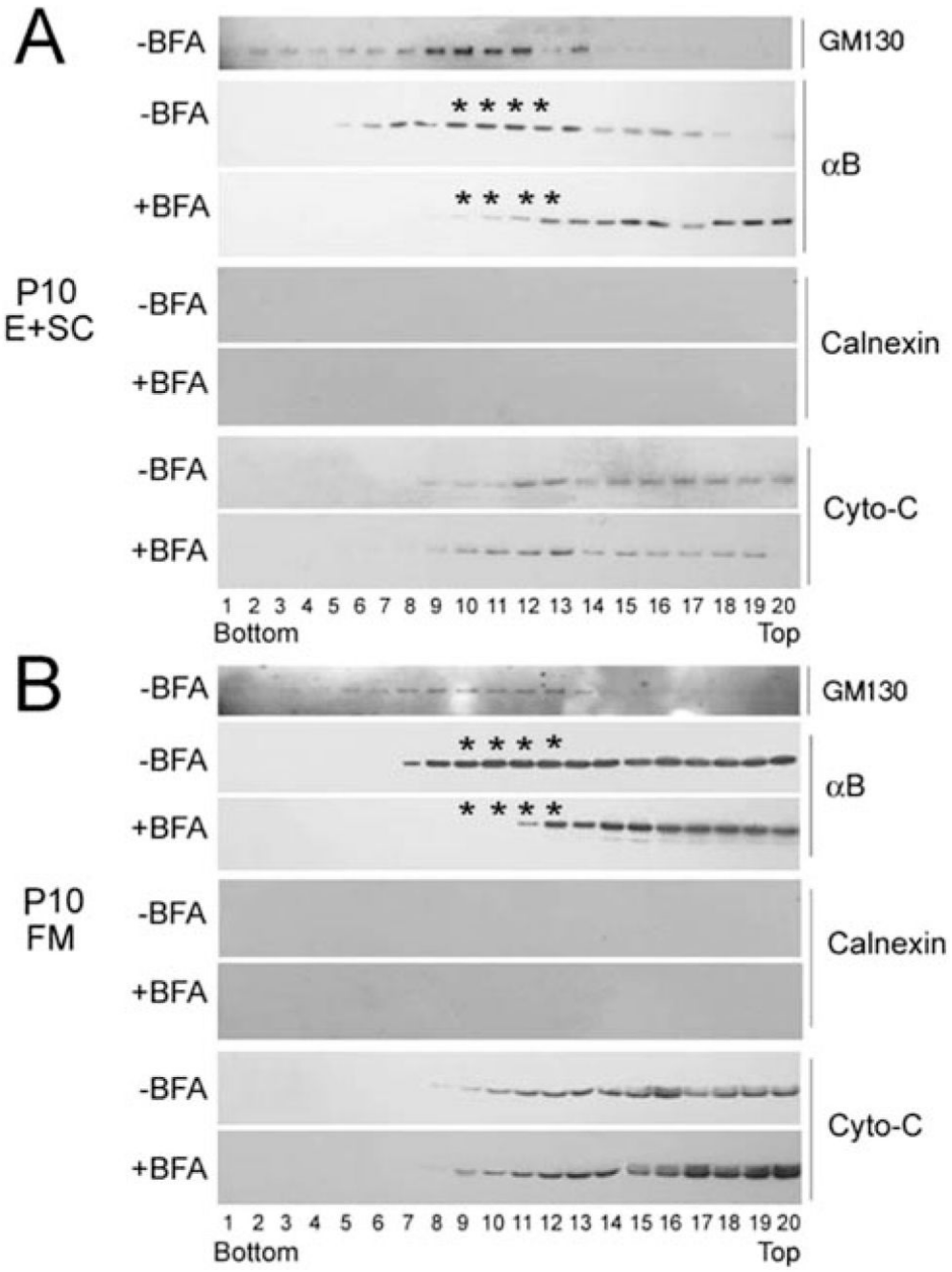

Figure 4.

Golgi membrane association of *α*B-crystallin is susceptible to BFA. The two anatomic domains, (**A**)E+SC (−BFA = 4.77 mg protein; +BFA = 2.62 mg) and (**B**) FM (−BFA = 6.01 mg; +BFA = 3.5 mg) were fractionated as described. The distribution of *α*B-crystallin in P10 lenses is similar to that obtained with P20 lenses. In E+SC gradients, note that the distribution of *α*B-crystallin changes, shifting to the top of the gradient on BFA treatment (**A**, +BFA). Similarly, a marked loss of Golgi-associated αB-crystallin is seen in the FM gradients (*asterisks*) (**B**, compare −BFA with +BFA). Calnexin (an ER marker) is undetectable, whereas there is no effect on the mitochondrial marker cytochrome *c* (Cyto-C). Only anti–GM130 immunoblots from −BFA are shown. GM130 is undetectable in +BFA gradients.

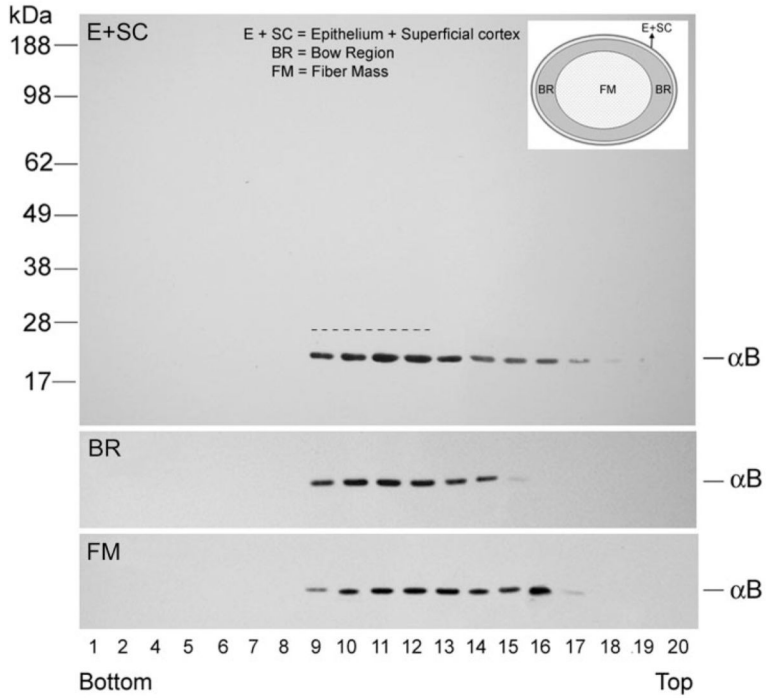

Figure 5.

αB-crystallin in P20 rat lens. Postnuclear homogenates obtained from three different regions of P20 rat lens (*inset*) were fractionated as described. Note that for E+SC, 524 μg total protein was loaded on the gradient compared with 8.40 mg and 10.00 mg for BR and FM, respectively. Thus, the BR and FM fractions had to be diluted 20× so that similar amounts of protein could be analyzed. Comparable amounts of protein (E+SC, 26.2 μg/fraction; BR, 21 μg/fraction; FM, 25 μg/fraction) were loaded on the gel to follow the distribution of αB-crystallin. A large proportion of αB-crystallin fractionates with the Golgi-enriched membrane in all three gradients (fractions 9–12, represented by the *dotted line* in the panel marked E+SC). *Top*: whole immunoblot with molecular mass standards. Only relevant areas are shown for the BR and FM panels.

NIH-PA Author Manuscript NIH-PA Author Manuscript NIH-PA Author Manuscript

NIH-PA Author Manuscript

NIH-PA Author Manuscript

NIH-PA Author Manuscript

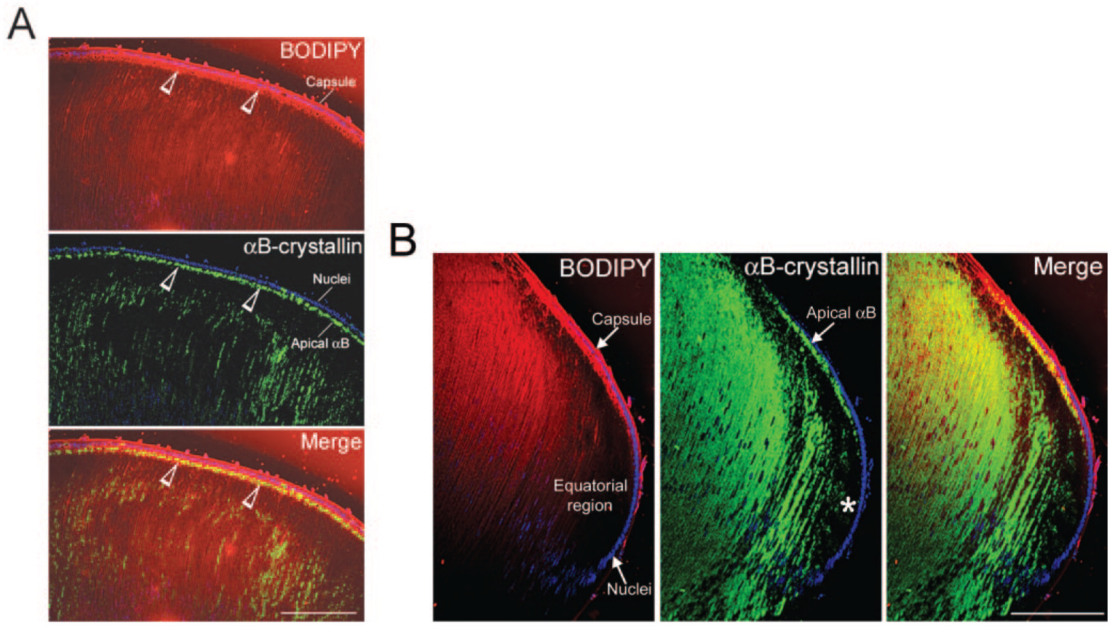

Figure 6.

Compartmentalized presence of αB-crystallin in the ocular lens. Confocal images of P10 rat lens sections labeled with ceramide (*red*) incorporated preferentially into Golgi lipids[27] and anti–αB-crystallin (*green*). Nuclei are stained with DAPI (*blue*). (**A**) Localization of αB-crystallin (*arrowheads*) in the apical epithelium. (**B**) Equatorial (bow) region of the P10 rat lens containing differentiating fiber cells stained with anti–αB-crystallin (*green streaks* running anterior-posterior along the length of the fiber cells). Note the lack of staining (*middle, asterisk*)atthe beginning of the bow region. Scale bar, 200 μm.

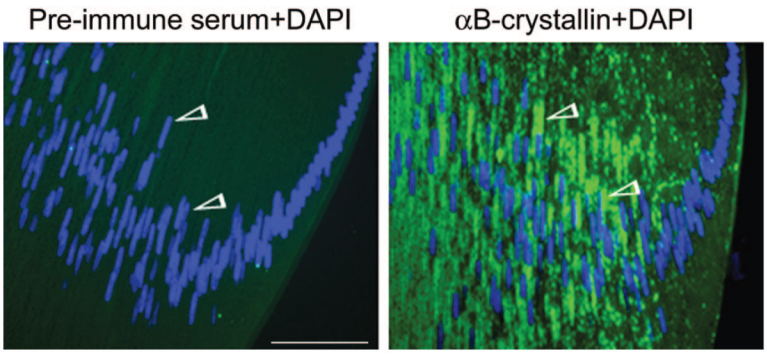

Figure 7.
Perinuclear Golgi stained with anti–αB-crystallin in differentiating fiber cells. Confocal images of the bow region of P10 lens (*right*) showing Golgi streaks (*green*, stained with anti–αB-crystallin, *arrowheads*) by the side of the elongating nuclei (*blue*). *Left*: control, without the primary antibody, showing elongating nuclei (*blue*, *arrowheads*). Scale bar, 100 μm.

NIH-PA Author Manuscript
NIH-PA Author Manuscript
NIH-PA Author Manuscript

NIH-PA Author Manuscript

NIH-PA Author Manuscript

NIH-PA Author Manuscript

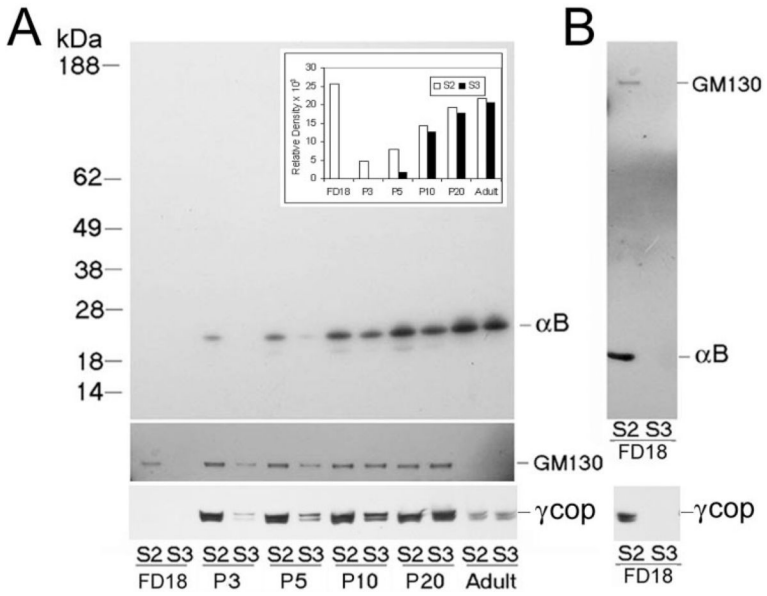

Figure 8.

Temporal study of the distribution of αB-crystallin in Golgi membrane and vesicular fractions in the developing lens. Postnuclear extracts were prepared from whole lenses of different ages and were analyzed on discontinuous sucrose density gradients (Fig. 3, *inset*). The Golgi membrane (S2) and vesicular membrane fraction (S3) were collected and diluted 1:10, and 1 μL was immunoblotted for αB-crystallin detection (**A**, *top*). No reaction was seen in the FD18 samples at this dilution, which were, therefore, immunoblotted again with 10 μL undiluted S2 and S3 fractions and probed sequentially with anti–αB-crystallin and anti-GM130 (**B**, *top*). The αB-crystallin immunoblot was scanned, and relative density values are presented in the bar graph (*inset*; FD18 values were taken from **B**). Note that the presence of αB-crystallin in the S3 fraction increases with developmental age. To establish that the S3 fraction contains Golgi-derived vesicles, two markers, GM130 and γCOP (a member of the COP1 coat protein complex involved in vesicle formation as part of the Golgi to ER transport) were followed.[23,26] The presence and absence of αB-crystallin in the S2 and S3 fractions are complemented by the presence and absence of GM130 and γCOP. For GM130 and γCOP, undiluted fractions (10 μL) were used for immunoblotting (only relevant areas of the immunoblots are shown). In the adult lens, GM130 is undetectable. That the extraction procedures do not unduly contribute to the generation of vesicles (fraction S3) is indicated by the lack of αB-crystallin in the S3 fraction in the younger lenses (**B**). The following protein amounts (μg/μL) from each fraction were used for immunoblotting: (**A**) S2/S3, F18, 0.25/0.19; P3, 0.97/0.38; P5, 1.44/0.70; P10, 1.63/0.54; P20, 1.49/1.08; Adult, 1.63/1.45. (**B**) S2/S3, 2.5/1.9. Although this is a qualitative analysis, we also analyzed equal protein amounts; the pattern did not show significant change.